Investigation of thermal characteristics of multitubial thermosyphon heat-exchangers

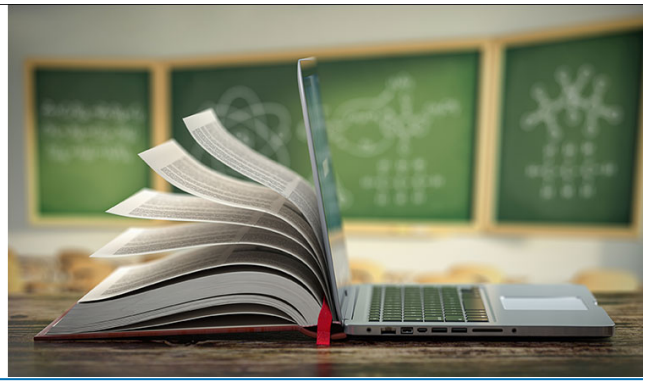

Investigation of thermal characteristics of multitubial thermosyphon heat-exchangers

L O Yakovlev[1], V A Klimova[1], S E Shcheklein[1]

[1]Ural Federal University, 19 Mira, 620002, Yekaterinburg, Russia

e-mail: leo00@mail.ru, v.a.klimova@urfu.ru, s.e.shcheklein@urfu.ru

Abstract. Prospects of application and advantages of heat-exchangers based on sealed two-phase thermosyphons are compared with analogies of alternative widespread designs. Theoretical limitations of heat transfer are considered. Experimental facility requirements were formulated. Heat transfer coefficients obtained by calculation, computer simulation and in experiments.

Key words: thermosyphon heat-exchanger, heat transfer coefficient, heat transfer efficiency improvement, experimental research, computational fluid dynamics.

1. Introduction

Although the subject has been well-studied in Russia and abroad, an in-depth investigation of thermosyphon heat exchanges application as a part of heat exchange modules within a temperature range used in utilities systems, heating and ventilation equipment such as domestic hot water (DHW) temperature boosters has, nevertheless, not been conducted. Currently, the plate-type and shell-and-tube heat-exchangers have been used mainly as DHW temperature boosters. The operating theory behind those devices is well-developed and design is close to perfect with the best models achieving a heat transfer coefficient of around 800 W/(m^2·K). Such high performance is usually achieved by increasing the medium flow velocity in the apparatus channels by decreasing their cross-dimension and that predetermines their main weakness – high sensibility to the water quality. Most often cold water supplied into the apparatus for heating is not treated and is saturated with salts and impurities. That leads to intense scaling, increased hydraulic resistance and lower heat exchange efficiency. Hence the heat-exchangers need purging up to 4 times a year to remove sediments and that is very a labor intensive and costly process which sharply increases running costs. Thermosyphon heat exchange design is free from these limitations and:

- An intermediate heat carrier boiling temperature can be set equal to a calculated temperature of the heated medium (for example 65°C for DHW) and that provides a sharp drop in scaling by bringing the temperature of the wall from the cold medium side down to a significantly lower level than the boiling temperature;
- Double medium separation provides increased reliability;
- High heat-transfer coefficient is maintained by small temperature drop;
- Heat carrier temperature control and adjustment are not required;
- Much more simple purging procedure allows to reduce operating costs.

2. Thermophysical limitations of heat transfer in the heat-exchanger

The main physical parameters of a vacuum thermosyphon qualitatively affecting its main characteristic (a power transfer) are [1]:

- Diameter to length of evaporating part ratio d/l_e which determines the size of space constraint influencing the boiling process;
- Working fluid (intermediate heat carrier);
- Thermosyphon inner pressure;
- Filling degree of a heating part.

There are also external factors influencing the heat-exchanger efficiency along with the internal features of heat-and-mass transfer inside the thermosyphon:

- Medium temperatures;
- Velocity and direction of flow around the tubes;
- Flow turbulization level.

Research was conducted on stainless steel thermosyphons having outer diameters of 20 mm and wall thicknesses of 1.5 mm. The assembly was vertically orientated and consisted of 4 working thermosyphons and 10 simulators made of heat insulating materials. The thermosyphon length was 1 m, consisting of an evaporating section of 0.7 m and a condensation section of 0.3 m. The absolute pressure inside the thermosyphon was 17 kPa and the calculated boiling temperature was 56°C.

2.1. Limiting heat flux in the thermosyphon' evaporating section

The functional connection between a limiting heat flow and a heating part geometry is well studied and validation is given in [1] based on our own results as well as that of others [2-6] and can be described as

$$q_F^l = 0{,}16 \cdot r \cdot \rho_s^{0,5} \cdot \left(\sigma \cdot g \cdot (\rho - \rho_s)\right)^{0.25} \cdot \left(1 - e^{-\frac{d}{l_e}\left(\frac{\rho}{\rho_s}\right)^{0.13}}\right)$$

where q_F^l – limiting heat flux through the thermosyphon heating surface, r – heat of evaporation, ρ_s – steam density, ρ – liquid density, σ – surface tension coefficient, g – gravity acceleration, d – thermosyphon diameter, l_s – length of thermosiphon evaporating section.

Thus, the limiting heat flux in the thermosyphon evaporating section with given parameters is q_F^l= 51.6741 kW/m^2, with a maximum power output of 1,955 kW for a single thermosyphon and $Q^e_{1\Sigma}$ = 7.822 kW for the thermosyphon assembly.

2.2. Maximum power output of the thermosyphon' condensation section

Following the conclusion [1] made by analysing a number of previous publications it is possible to apply Nusselt's Theory of Film Condensation with provision for the Reynolds number for calculating the heat transfer coefficient during condensation inside a thermosyphon.

An average heat transfer coefficient is $\alpha_c = 6053$ W/(m^2·K) which agrees with the results obtained by other researchers [7].

Hence, the maximum power output of the thermosyphon condensation section will be 5.9 kW while the maximum power output of the thermosyphon assembly will be $Q^c_{1\Sigma}$ =23.6 kW.

However, according to more recent data, a condensation process in a thermosyphon takes place under different conditions than those occurring under Nusselt's experiments, and that leads to a lowering of the local Nusselt's number by almost an order of magnitude [8]. An acceptable theory to describe that process has yet to be developed so we applied a general conclusion and used Nu and consequently α_c and Q_c as in [8].

Then for the assembly under consideration we have α_c = 605 W/(m^2·K), Q_{c1} = 0.59 kW, $Q^c_{\text{пр}\Sigma}$ = 2,36 kW.

2.3. Maximum power output of thermosyphon by external limitations

The internal process parameters for the thermosyphons under consideration do not change, unlike external heat-exchange which is defined by the regime of flow i.e. by direction and velocity of flow at each surface point. Typical medium flow variants are:

- longitudinal medium motion along the thermosyphons (see Figure 1)

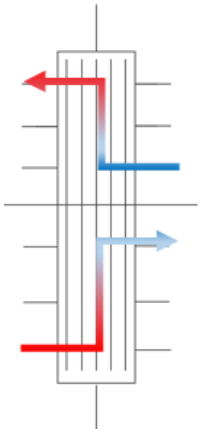

Figure 1. Diagram of longitudinal medium flow in thermosyphons.

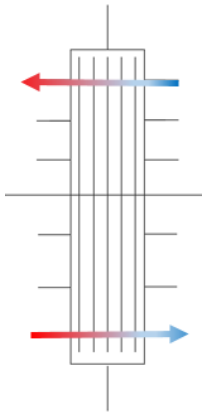

Figure 2. Diagram of cross flow in thermosyphons.

For that regime of flow, we can use the calculation method as for shell-and-tube heat-exchangers [9]:

$$\alpha = 1{,}16 \cdot \left(1210 + 18t_{av}^{int} - 0{,}038\left(t_{av}^{int}\right)^2\right) \cdot \frac{W_{int}^{0.8}}{d_{eq}^{0.2}},$$

where: 'int' is an intertubular space, d_{eq} – equivalent diameter of intertubular space, W_{int} – water velocity in intertubular space, t_{av}^{int} – average water temperature in intertubular space.

Table 1. Power output of a heat-exchanger with longitudinal medium flow.

Volume flow,	Power of evaporating and condenser part			
L/s	Q_e, W	Q_c, W	$Q_{e\Sigma}$, W	$Q_{s\Sigma}$, W
0.1	281.95	122.10	1127.78	488.40
0.2	490.90	212.59	1963.58	850.35

- medium motion across the tube bundle (see Figure 2)

In that case, heat transfer can be described by [7]:

$$\overline{Nu}_{ld} = 1.8 \cdot Re_{ld}^{\frac{1}{3}} \cdot Pr_l^{\frac{1}{3}} \cdot \left(\frac{Pr_l}{Pr_w}\right)^{\frac{1}{4}}$$

where the liquid is «l» and the thermosyphon wall is «w».

Table 2. Power output of a heat-exchanger with cross flow of medium.

Volume flow,	Power of evaporating and condenser part			
L/s	Q_e, W	Q_c, W	$Q_{e\Sigma}$, W	$Q_{s\Sigma}$, W
0.2	819.78	347.47	3279.10	1389.89

2.4. Computer simulation for the thermosyphon power output

FlowSimulation software was used for simulation under the following conditions:

- no temperature losses through the body frame;
- thermosyphons are simulated as rods of infinite heat conductivity.

Figure 3 shows velocities and trajectories of the liquid motion in the body of the heat-exchanger.

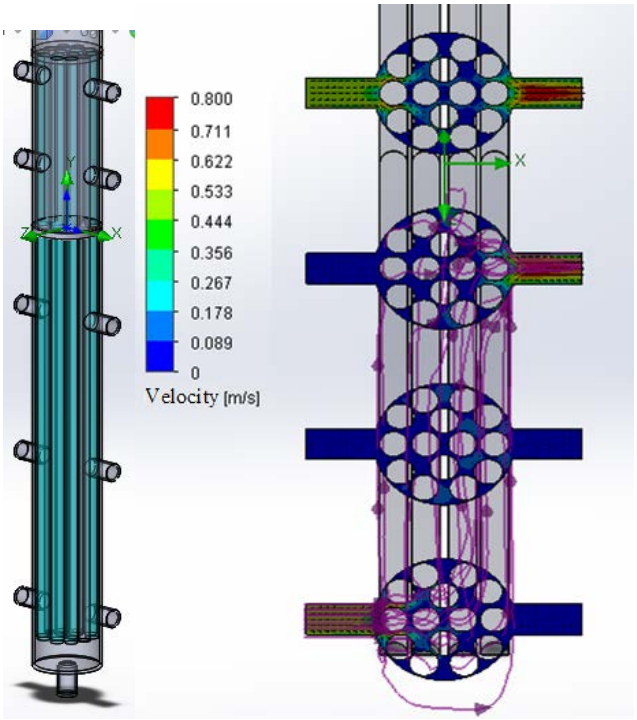

Figure 3. Simulation results at the volume flow rate 0.23 L/s.

Table 3 shows quantitative results of calculation of the heat transfer coefficient for thermosyphons with different orientation inside the heat-exchanger body.

Table 3. Simulation results for heat transfer coefficient, W/m^{2}K.

Flow 0.1 L/s						
Tube №	Condenser			Evaporator		
	min	Surface averaged	max	min	Surface averaged	max
1	26.3	409.2	3863	11,5	114.9	998.2
2	0.2	566.2	4015.7	12,3	145.3	4068.5
3	0	593.2	5681.6	7,9	149.3	2964.5
4	0	687.8	9143.7	16,1	153.05	1880.5
Average		**564.1**			**140.6**	
Flow 0.2 L/s						
Tube №	Condenser			Evaporator		
	min	Surface averaged	max	min	Surface averaged	max
1	63.9	584.8	3858.7	16.9	142.3	4220.7
2	0.6	983.4	5948.1	12.2	191.6	5210.2
3	21.9	894.4	6370.7	11.5	181.7	3986.7
4	1.86	1142.2	7583.1	15.8	190.8	2935.8
Average		**901.2**			**176.6**	

2.5. Experimental research of the heat-exchanger heat transfer coefficients and power output

Readings were taken under stable conditions; the duration of each measurement was 3 min and reading recording rates were one per second.

Figures 4 and 5 show pictures and diagrams of the thermosyphon assembly and test console.

Temperature was measured using platinum thermal elements of Pt100 type first class and registered by the hardware and software suite. Water flow from both heating and heated circuits side was measured by high accuracy water meters. The pressure in the thermosyphon was calibrated using test pressure gauges–vacuum meters.

a b

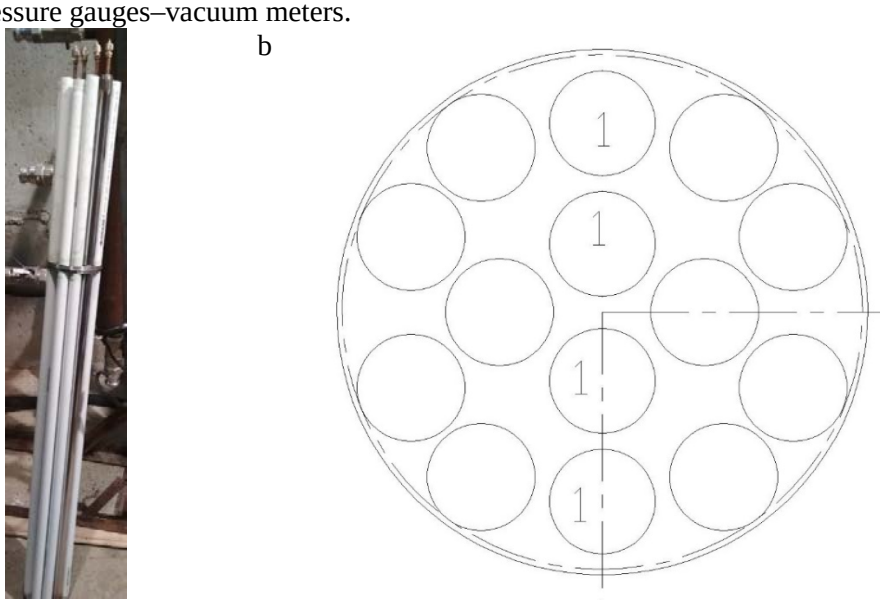

Figure 4. Thermosyphon assembly

a b

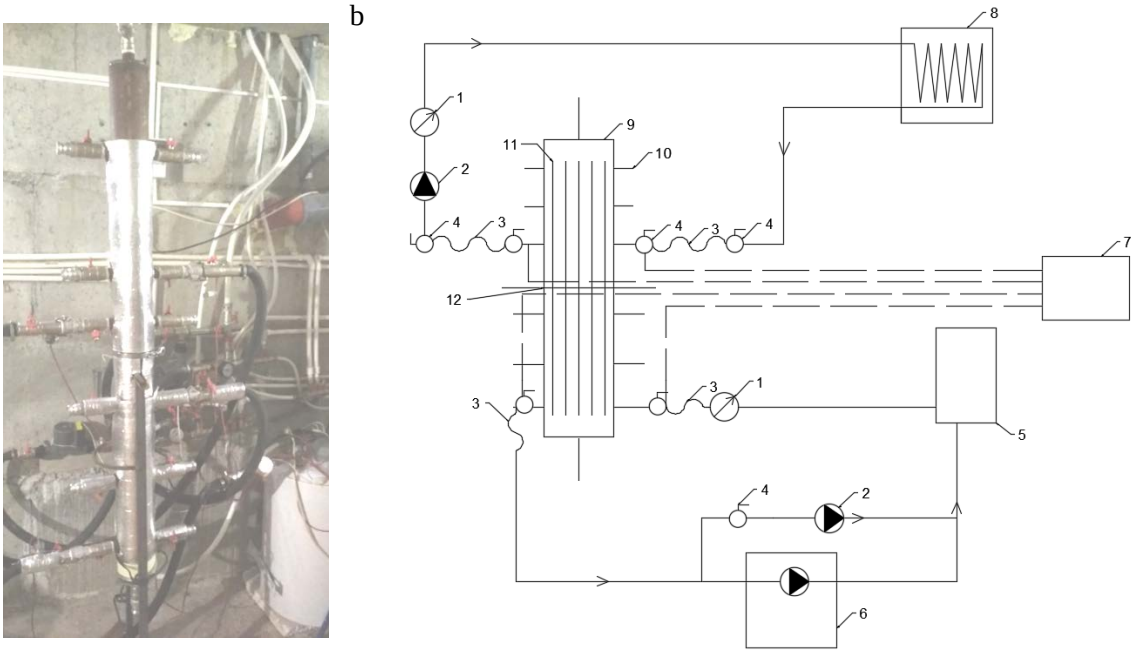

Figure 5. The process flow diagram of test console.
1 – Water flow meter, 2 – Circular water pump, 3 – Flexible hose with quick release connections, 4 – Ball tap, 5 – Insulated heat storage, 6 – Heat source (gas boiler), 7 – Hardware and software suite for registering temperature readings, 8 – Cooling system based on Aluminium radiators, 9 – Heat-exchanger body frame, 10 – Connection port, 11 – Thermosyphon (or simulator), 12 – Quick release body connection.

Table 4. Experimental values of temperatures, power output and heat transfer coefficients.

Flow, L/s	Evaporator	0.1	0.1	0.18	0.2	0.23	0.1	0.2
	Condenser	0.1	0.2	0.18	0.2	0.23	0.59	0.59
Average water temperature of evaporator, °C		67.68	65.65	63.73	62.58	68.02	64.88	63.84
Average temperature drop in evaporator °C		11.68	9.65	7.73	6.58	12.02	8.88	7.84
Average water temperature of condenser, °C		26.13	26.43	26.77	26.94	27.48	27.50	27.33
Average temperature drop in condenser, °C		29.87	29.57	29.23	29.06	28.52	28.50	28.67
Power output Q, kW		1.36	1.79	1.68	1.77	1.89	1.91	2.79
Heat transfer coefficient α, W/(m^2·K)	Evaporator	0.93	1.09	1.45	1.61	1.06	1.54	1.47
	Condenser	0.60	0.80	0.76	0.81	0.88	0.89	1.29

3. Conclusions

Table 5 shows a comparison of the thermosyphon heat-exchanger power output values obtained by calculation, computer simulation and experimental research.

Table 5. Summary table.

Flow, L/s	Evaporator	0.1	0.1	0.2	0.2
	Condenser	0.1	0.2	0.2	0.59
Power output, kW	With limitations in evaporator	7.822			
	With limitations in condenser according to [8]	2.36			
	With external limitations of evaporator	1.13	1.13	1.96	1.96
	With external limitations of condenser	1.08	1.39	1.39	2.04
	With computer simulation	1.27		1.77	
	With experimental research	1.36	1.79	1.77	2.79

Clearly, the thermosyphon heat-exchanger demonstrates high performance: heat-exchanger power output shows little dependency on temperature drop and goes over the theoretical limit calculated by using existing equations on external flow conditions. It also goes above the internal limitations described in [8] and matches the computer simulation results.

References

[1] Pioro I, Antonenko V, Pioro L 1991 Efficient heat-exhcangers with two-phased thermosyphons (Ukraine: Naukova Dumka) 245 p.

[2] Bezrodnyi M 1977 Affect of intermediate heat-carrier pressure on critical heat flow in evaporating thermosyphons *USSR. VUZ bulletin. Energetika,* pp 80-84

[3] Stoyanov N Critical heat flux inside closed evaporating thermosyphons 1987 *USSR Engineering and Physics Journal* **53** **№1**. pp. 20-26.

[4] Bezrodnyi M 1979 Investigation of maximum heat flows in tilting evaporating thermosyphons *USSR. VUZ bulletin. Energetika* **№4.** P. 110-112

[5] Savchenkov G, Kunakov V Research of critical heat flux inside low-temperature evaporating thermosyphons *1978 USSR. Engineering and Physics Journal*. **35**, **№3**. pp 397-404.

[6] Bezrodnyi M 1978 About upper limit of the maximum heat-carrier power of evaporating thermosyphons *USSR Teploenergetika Journal* **№8**. pp 63-66.

[7] Isachenko V, Osipova V, Sukomel A 1982 Heat Transfer: coursebook for universitites (Moskow: Egergoizdat) 416 p.

[8] Pashkevitch R, Muratov P 2014 Research on film-type condensation in vertical tubes with upwardy moving steam *Mining informational and analytical journal* (scientific and technical journal).

[9] SP 41-101-95. Boiler house design.